

Effect of Nucleation of Poly(1,4-butylene terephthalate) on Its Flowability[†]

Yasuhiko ONISHI and Tasuku NAKAI*

Sumitomo Wiring Systems, Ltd., Suzuka 513, Japan

*Hiroshima Institute of Technology, Hiroshima 731-51, Japan

(Received December 28, 1990)

ABSTRACT: The induction time t_0 in nucleation of poly(1,4-butylene terephthalate) (PBT) was measured and its effect on solidification time t_s of melted PBT was studied. When two samples of PBT-A and PBT-B composed of different molecular weight were mixed together to prepare sample PBT-C and then melted, the induction time became longer in comparison with individual samples. The thermodynamic consideration was applied for the clarification of such behaviour. As the result of consideration, it was found that the enthalpy change at melting ΔH_m of sample PBT-C became higher than individual samples and the flowability of sample PBT-C became four times higher in comparison with both samples.

KEY WORDS High Flowability / Poly(1,4-butylene terephthalate) / Primary Nucleation / Induction Time / Nucleation Theory /

PBT has superior mechanical properties as industrial material and engineering thermoplastics due to its rapid solidification and mouldability.¹ The output of such PBT is increasing rapidly as a new material for electro connectors.

However, it has been well-known that PBT is inferior in the flowability at moulding and the elasticity at low temperature. Such undesirable properties lead to its high solidification rate at moulding. Generally, PBT has a higher solidification rate than poly(ethylene terephthalate) (PET) obtained in the lower degree of crystallinity.^{2,3}

In this study, the properties of three kinds of PBT, that is, PBT-A and B having weight average molecular weight of 45900, and 61800, respectively and PBT-C composed of both the PBTs in equal quantity, were examined. The solidification mechanism was also discussed thermodynamically.

EXPERIMENTAL

Material

Two kinds of PBT-A and B, determined as having weight-average molecular weight of 45900 ($\bar{M}_w/\bar{M}_n=2.2$) and 61800 ($\bar{M}_w/\bar{M}_n=2.2$) using intrinsic viscosity $[\eta]=7.39 \times 10^{-5} \bar{M}_w^{0.871}$,⁴ were used. PBT-A and B showed the same IR spectrum. PBT-C was prepared by the mixing in equal quantity of PBT-A and B and the keeping melt at 543 K for 5 minutes. The intrinsic viscosity $[\eta]$ [$\text{cm}^3 \text{g}^{-1}$] $\times 10^{-3}$] of PBT-A and B measured in tetrachloroethane-phenol (40:60) mixture at 303 K was 0.85 and 1.10, respectively. The thermal properties of PBT at melting will be shown later in Table II.

Measurement by Optical Absorption

Three kinds of dried PBT powder were moulded using the Mettler FP-80 hot stage attached to a Nikon polarizing microscope.

[†] A preliminary report of this work was presented at the Ninth International Conference on Crystal Growth held on 20th—25th August 1989, Sendai, Japan.

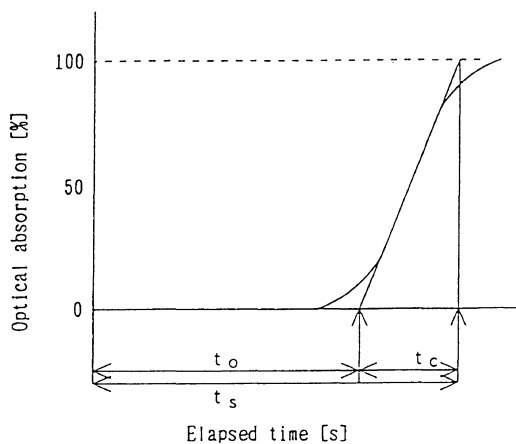


Figure 1. The solidification scheme. t_0 , induction time; t_c , growth time; t_s , solidification time.

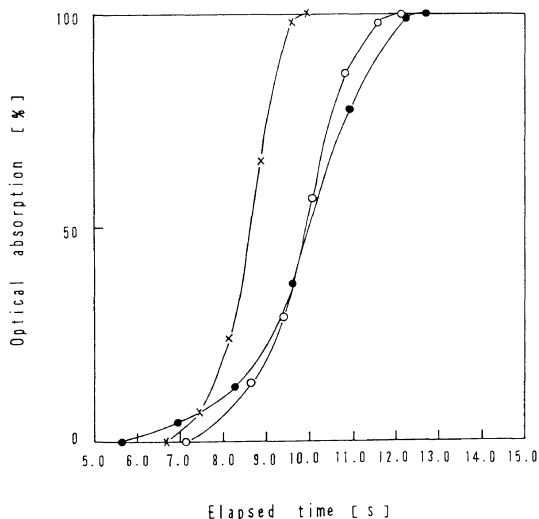


Figure 2. The formation time of nuclei and solidification time of PBT. —x—, PBT-A; —●—, PBT-B; —○—, PBT-C.

PBT samples were pressed between the microscope cover glasses and thereafter melted through heating at 543 K for 3 min. The melted samples were moved to another hot stage held at 343 K to solidify. The formation rate of nuclei⁵ and the solidification time*¹ of PBT were determined by optical absorption. A

Table I. Induction time of nucleation t_0 , growth time of nuclei t_c , and solidification time t_s

Sample	Induction time, t_0	Growth time, t_c	Solidification time, t_s
	s	s	s
PBT-A	7.7	1.6	9.3
PBT-B	8.3	3.2	11.5
PBT-C	8.7	2.3	11.0

typical solidification scheme is shown in Figures 1 and 2.

After the induction time for primary nucleation t_0 , the optical absorption increased suddenly due to primary nucleation, and afterwards continued the linear change with elapsed time which corresponded to growth time t_c . The average values of these data obtained through three experimental runs are listed in Table I. The deviation of measured times in each experimental run was within $\pm 1.5\%$ of the mean values.

Calculation of Crystallinity through Density Measurement

The density measurement for the calculation of crystallinity was carried out by the density gradient column, using two solutions of carbon tetrachloride and isopropyl alcohol. The crystallinity in weight fraction X of solidified PBT was calculated by the following relationship⁶:

$$X = \rho_c(\rho - \rho_a) / \rho(\rho_c - \rho_a) \quad (1)$$

where ρ_c , ρ_a , and ρ [g cm^{-3}] are densities of crystalline PBT (1.396),⁷ amorphous PBT (1.278),⁸ and samples obtained in this experiment. The numerical values of X thus calculated are listed in Table II.

Thermal Analysis

The differential scanning calorimetry using a Rigaku DSC 8230 was used to measure 10 mg

*¹ Solidification time t_s was defined as the sum of t_0 and t_c as shown in Figure 1.

Table II. Melting temperature T_m , melting peak temperature T_{pm} , heat of fusion ΔH , weight fraction crystallinity X , and, enthalpy change at solidification ΔH_m

Sample	T_m K	T_{pm} K	ΔH J g ⁻¹	X	ΔH_m J g ⁻¹
PBT-A	488.2	496.2	56.1	0.342	164.0
PBT-B	488.2	496.6	51.9	0.315	164.8
PBT-C	488.1	496.4	67.4	0.307	219.2

of powder samples packed into an aluminium pan at the heating rate of 10 K min⁻¹. The average values of these data obtained through three experiment runs are listed in Table II. The deviation of measured values in three runs was within $\pm 1.5\%$ with the mean values.

Measurement of Infrared Absorption

The IR measurement with PBT-A, B, and C were carried out by the KBr method.

THEORY

The total solidification time t_s [s] of melted PBT is defined as follows⁹:

$$t_s = t_o + t_c \quad (2)$$

where t_o [s] is the induction time for primary nucleation and t_c [s] is the growth time of primary nuclei, till the completion of solidification based on two-dimensional nucleation on the surface of growing nuclei. As shown in Table I, it is clear that t_o of PBT was comparatively longer than t_c . From these experimental data, the following fact became clear that the solidification time of PBT was controlled by the primary nucleation process. After the induction time, the primary nuclei were formed slowly and then the growth of PBT nuclei proceeded very quickly.

The relationship between the formation rate of primary nuclei J [s⁻¹] and the induction time t_o can be expressed as follows¹⁰:

$$J \propto 1/t_o \quad (3)$$

Usually, such a rate process can be written as

the following equation,¹⁰ using activation energy Δg_n .

$$J = k' \exp(-\Delta g_n/kT) \quad (4)$$

where k' [s⁻¹] is nucleation rate constant, k [J K⁻¹] Boltzmann constant and T [K] absolute temperature at nucleation.

The Gibbs free energy change Δg_n at primary nucleation is expressed as the difference of surface and bulk Gibbs free energies⁵

$$\Delta g_n = 4\pi r^2 \sigma - nkT\Delta T^* \quad (5)$$

where r [cm] is the radius of nucleus, σ [J cm⁻²] is the surface energy of the nucleus, n is the number of PBT molecules composed of nucleus, $\Delta T^* = (T_m - T)/T_m$ is the degree of supercooling temperature, and T_m [K] is the melting point of PBT. The first and second terms of the right side in eq 5 express Gibbs energy changes based on the appearance of nucleus surface and phase change from melt to solid, respectively.

Although the radius r changes by the growth and dissociation based on molecular motion, a stable nucleus is formed under the condition of $d\Delta g_n/dr = 0$. Therefore, the radius and Gibbs free energy change for critical nucleus can be decided as the radius of critical nucleus r_c [cm] at $d\Delta g_n/dr = 0$, and the corresponding Gibbs free energy change Δg_n [J] for the case of the formation of critical nuclei in melted polymer¹⁰:

$$r_c = 2\sigma v/kT\Delta T^* \quad (6)$$

$$\Delta g_c = (16/3) \cdot \pi \sigma^3 (v/kT\Delta T^*)^2 \quad (7)$$

where v [cm^3] is the average volume of PBT molecules.

When the radius of nucleus formed in melted PBT grows into r_c , the nucleus becomes stable and begins the growth to crystal. Accordingly, the nucleation rate J can be expressed as the rate process which has the activation energy Δg_c

$$J = k' \exp\left\{-\frac{(16/3)\pi\sigma^3(v/kT\Delta T^*)^2}{kT}\right\} \quad (8)$$

The induction time of primary nucleation t_0 can be expressed as follows:

$$t_0 = (k')^{-1} \exp\left\{\frac{(16/3)\pi\sigma^3(v/kT\Delta T^*)^2}{kT}\right\} \quad (9)$$

If the surface energy of nucleus σ increases, r_c becomes larger and t_0 becomes longer as shown in eq 8 and 9, respectively.

Referring to the theory mentioned above, it becomes clear that the solidification time t_s of PBT can be elongated by the increase in surface energy σ of PBT nucleus. Such a longer solidification time means a good flowability of PBT at moulding process.

RESULTS AND DISCUSSION

Table I shows the induction time of primary nucleation t_0 , growth time of nuclei t_c and solidification time t_s for PBT-A, B, and C. As shown in Table I, the induction time t_0 of PBT-C becomes longer compared with PBT-A and B composed of polymeric chains with different weight average molecular weight of 45900 and 61800, intrinsic viscosity of 0.85 and 1.10, respectively. The growth time t_c is depending on the molecular weight in the order of $B > C > A$. Therefore, the solidification times t_s , being the sum of t_0 and t_c , are in the order of $B > C > A$.

Although the viscosity of melted PBT is low till the primary nucleation, it increases abruptly by the initiation of the primary nucleation.

Therefore, PBT, which has the moderately longer induction time, is suitable for the moulds consisting of small and complicated cavities. For the case of short induction time, the melted PBT increases the viscosity before the complete injection into cavities.

Because the viscosity of solidifying PBT increases suddenly after the primary nucleation and the flowability of melted PBT is hindered after the primary nucleation, the elongation in t_0 is more important from the viewpoint of flowability. Accordingly, the larger value in t_0 , as in the case of PBT-B, is undesirable at moulding process.

From the injection moulding experiments, it was clearly confirmed that PBT-C had four times higher flowability in the industrial mould.*² Namely, the same flowability was obtained for PBT-C in the case of supercooling larger than PBT-A.

Figure 3 shows DSC chart of PBT-A, B and C in which the melting endotherm peaks are observed at the vicinity 496 K. Table II shows the melting temperature T_m , melting peak temperature T_{pm} , heat of fusion ΔH [J g^{-1}], weight fraction crystallinity X , and enthalpy change at solidification ΔH_m *³ [J g^{-1}].

Although the melting temperatures T_m are almost constant in the range of 488.1–488.2 K, PBT-C has higher ΔH and ΔH_m than PBT-A and B. Such experimented results mean that the intermolecular force in PBT-C molecules arranged as crystalline structure is the largest among the three PBT.

From the viewpoint of thermodynamics for the solidification of PBT, the Gibbs free energy change at solidification ΔG [J g^{-1}] can be written as follows:

$$\Delta G = \Delta H_m - T_m \Delta S_m \quad (10)$$

where ΔS_m [$\text{J g}^{-1} \text{K}^{-1}$] is the entropy change at solidification. When the solid-liquid equi-

*² Flowability was evaluated by the injection temperature to be able to mould by means of an industrial mould, using the relationship between melt viscosity and its temperature.¹²

*³ $\Delta H_m = \Delta H/X$. ΔH_m is the total enthalpy change at solidification for the case of a perfectly crystalline form.

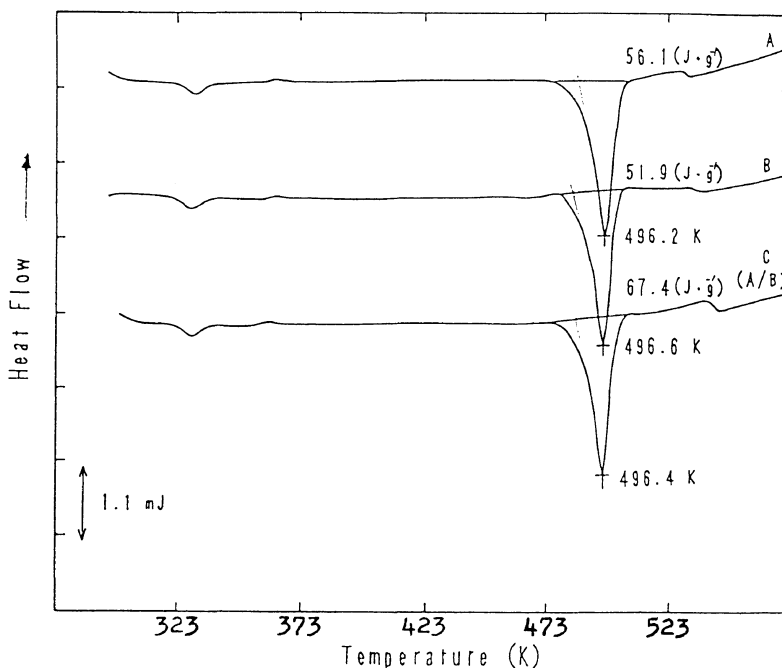


Figure 3. DSC chart of PBT-A, B, and C.

librium is attained,*⁴ ΔG becomes zero, and the following relationship can be derived.

$$T_m = \Delta H_m / \Delta S_m \quad (11)$$

Because T_m is almost constant for the present experiments, ΔS_m changes proportionally with the ΔH_m change at the solidification through the primary nucleation.

ΔH_m of PBT-C is the largest compared with the other two PBT's, and therefore ΔS_m of PBT-C becomes the largest. The larger ΔS_m also means the wider size distribution of molecular weight of polymeric chains in PBT. Such an inference is considered to be reasonable, considering that PBT-C is prepared by the mixing of PBT-A and B.

The large ΔH_m means that the PBT molecules in a crystal structure are more strongly packed by the intermolecular force, and then the increase in surface energy may be expected in the case of such a crystal structure.

PBT-A, B, and C in Table II are considered as α -type PBT because of their melting temperatures at the vicinity of 488 K, but PBT-C is considered to have a different intermolecular structure. Figure 4 shows IR spectra of PBT-A, B, and C which show the spectrum of $-\text{CH}_2$ stretching vibration at $800\text{--}900\text{ cm}^{-1}$. There are observed small differences in PBT-C, in comparison with PBT-A and B, which are classified as α type PBT.¹³ PBT-C has a similar spectrum as β type PBT, in that a crystal packing is improved for its zigzag CH_2 chains arranged more closely.^{13,14} Considering such an experimental result, zigzag CH_2 chains in PBT-C may be arranged more closely by their intermolecular force, which occurred through the interchange reaction between PBT-A and B, which was proposed by Flory.¹⁵⁻¹⁸

Referring to eq 7, it becomes clear that the Gibbs free energy change at the primary

*⁴ Such a state is considered to correspond to the boundary between metastable and labile zones.

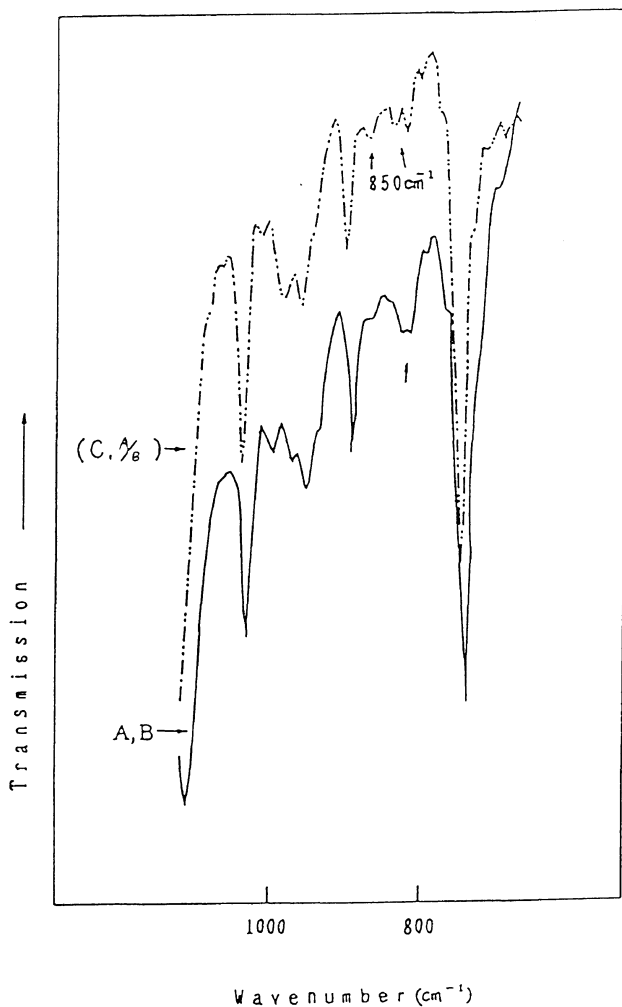


Figure 4. IR spectra of PBT-A, B, and C.

nucleation Δg_c increases proportionally with the third power of surface energy σ . According to such a thermodynamic relationship, it becomes clear that the induction time t_0 increases with the increase of surface energy σ , as shown by eq 9. The surface energy of PBT nucleus, when it comes in contact with melted PBT, is expressed as the difference of intermolecular forces between liquid and solid states of PBT.

This difference of intermolecular force also corresponds to the enthalpy change at the melting represented as ΔH or ΔH_m at

solidification. Because the phenomenon of the primary nucleation is focused only on the crystalline nucleus, ΔH_m value is more important for the estimation of induction time t_0 . As mentioned above, the reason for the high flowability of PBT-C can be understood satisfactorily in respect to the increase of σ .

Figure 5 shows the micrographs from the polarizing microscope of the smallest spherulites in the slice samples of PBT-B and C by microtome. PBT-B has an almost uniform matrix composed of about $1\mu\text{m}$ grain size, while PBT-C has the larger grain size of

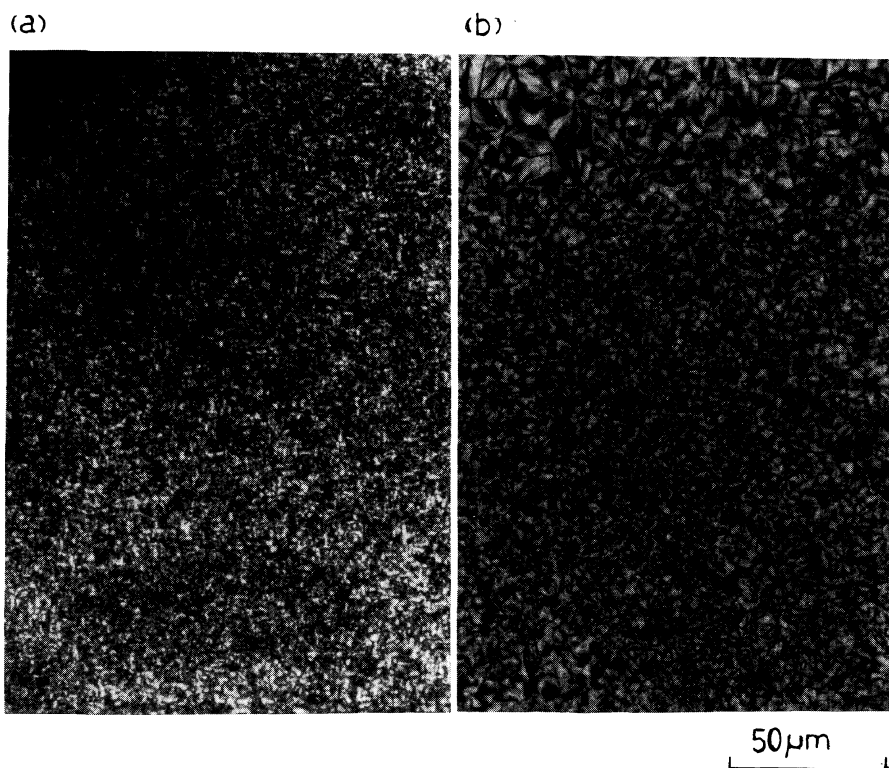


Figure 5. Polarizing micrographs showing the smallest spherulites in the slice sample of PBT-B and C by a microtome. (a) PBT-B and (b) PBT-C (A : B = 1 : 1).

2—10 μm . This difference in matrix can be also connected with the increase of the critical nuclei radius r_c expressed by Equation 6 and with the increasing of surface energy σ of a formed nuclei.

As the result of the consideration for the enthalpy change at solidification, it will be concluded that the surface energy σ between nucleus and melted PBT-C is the largest, and induction time also becomes the largest. But, the microscopic behavior at solidification has not been clarified at present.

CONCLUSIONS

The moulding properties for three kinds of PBT used mainly as electroconnector were measured. As a result of the experiment and the theoretical considerations, the following

novel facts were clarified.

(1) The induction time at solidification was the longest for PBT-C, composed of PBT-A and B in equal quantity, than two individual PBT's.

(2) The enthalpy changes between melted and crystalline PBT were the largest for PBT-C.

(3) The surface energy of the nucleus, which appeared at the interface with the melted PBT, was supposed to be the largest for PBT-C, on the basis of the consideration of the nucleation theory.

Acknowledgments. The authors are grateful to Mr. Yoshio Matsuda, the managing director of Sumitomo Wiring Systems, Ltd., for his continuing support. The authors also thank Miss Miyuki Odama and Miss Minako Tanaka, for their IR and DSC measuring.

REFERENCES

1. W. F. H. Borman and M. Kramer, *Am. Chem. Soc. Org. Coat. Plast. Chem., Paper*, **34**, 77 (1974).
2. M. Gilbert and F. J. Hybart, *Polymer*, **13** 327 (1972).
3. C. F. Pratt and S. Y. Hobbs, *Polymer*, **17**, 12 (1976).
4. W. F. H. Borman, *J. Appl. Polym. Sci.*, **22**, 2119 (1978).
5. Y. Harano, *Kagaku Kogaku*, **40**, 476 (1976).
6. R. S. Stein and A. Mirsa, *J. Polym. Sci., Polym. Phys. Eds.*, **18**, 327 (1987).
7. C. A. Boye, Jr. and J. R. Overton, *Bull. Am. Phys. Soc.*, **19**, 352 (1974).
8. S. Y. Hobbs and C. F. Pratt, *J. Appl. Polym. Sci.*, **19**, 1701 (1975).
9. G. W. Preckshet and G. G. Brown, *Ind. Eng. Chem.*, **44**, 1314 (1952).
10. I. Gutzow, V. Dochev, E. Pancheva, and K. Dimov, *J. Polym. Sci., Polym. Phys. Ed.*, **16**, 1155 (1978).
11. F. P. Price, in "Nucleation," A. C. Zettlemoyer, Ed., Marcel Dekker, New York, N.Y., 1969, Chapter 8.
12. K. Uki, Ed., "Houwa-poriesuteru-jushi Handobukku," Vol. 1, Nikkankogyo, Tokyo, 1989, p 326.
13. K. Tashiro, Y. Nakai, M. Kobayashi, and H. Tadokoro, *Macromolecules*, **13**, 137 (1980).
14. M. Yokouchi, Y. Sakakibara, Y. Chatani, H. Tadokoro, T. Tanaka, and K. Yoda, *Macromolecules*, **9**, 266 (1976).
15. M. Imoto, "Koubunshi-seiseino-Kagaku," 4th ed, Asakura Shoten, Tokyo, 1958, p 197.
16. P. J. Flory, *J. Am. Chem. Soc.*, **64**, 2205 (1942).
17. P. J. Flory, *J. Chem. Phys.*, **12**, 425 (1944).
18. P. J. Flory, "Principles of Polymer Chemistry," Cornell University Press, Ithaca, N.Y., 1953, p 70.